Available online at www.sciencedirect.com
SCIENCE DIRECT®
Materials Research Bulletin 39 (2004) 2035–2048
Materials Research Bulletin
www.elsevier.com/locate/matresbu

Influence of pH on the sorption behaviour of uranyl ions in mesoporous MCM-41 and MCM-48 molecular sieves

K. Vidya[a], N.M. Gupta[b], P. Selvam[a,*]

[a]*Department of Chemistry, Indian Institute of Technology-Bombay, Powai, Mumbai 400076, India*
[b]*Applied Chemistry Division, Bhabha Atomic Research Centre, Trombay, Mumbai 400085, India*

Received 30 September 2003; received in revised form 15 July 2004; accepted 21 July 2004

Abstract

The sorption of uranyl ions in mesoporous MCM-41 and MCM-48 was accomplished with the help of a direct-template-exchange route, and the progress was monitored as a function of pH of the precursor uranyl nitrate solution. Under identical conditions of synthesis, around one and a half times larger amount of uranium was found to be sorbed in MCM-48 (~12.5 wt.%) as compared to MCM-41 (~9.5 wt.%). Further, the powder X-ray diffraction (XRD) data revealed that the expansion of unit cell parameters and broadening of reflections of the uranium containing samples depended on the pH of the precursor uranyl solution. Likewise, the Fourier transform infrared spectroscopy (FT-IR) studies showed a progressive decrease in the frequency of the axial O=U=O asymmetric stretching vibrational band, ν_a(U=O) of the anchored uranyl groups with the increase of pH of the exchanging uranyl solution. The presence of two bands at ~920 and 879 cm^{-1} for uranyl exchanged samples prepared at pH > 5 indicated the presence of trinuclear $(UO_2)_3(OH)_5^+$ species. The occlusion of uranium thus depends upon the pore structure of the host material and the nature and dimension of the hydrolysis species formed at a particular pH of uranyl solution. Furthermore, the template-exchange of hexavalent uranium in MCM-41 and MCM-48 not only results in the formation of bulky hydrolysis species in the mesovoids, but also substitutes (isomorphously) in the silicate matrix resulting in the formation of UMCM-41 and UMCM-48.

Keywords: A. Inorganic compounds; B. Chemical synthesis; C. X-ray diffraction; D. Infrared spectroscopy

* Corresponding author. Tel.: +91 22 25767155; fax: +91 22 25767152.
E-mail address: selvam@iitb.ac.in (P. Selvam).

0025-5408/$ – see front matter © 2004 Elsevier Ltd. All rights reserved.
doi:10.1016/j.materresbull.2004.07.013

1. Introduction

The entrapment of uranyl ions in various zeolites and molecular sieves has been investigated, with attention being particularly directed towards their potential use as photocatalysts [1,2] and catalysts in the thermal degradation of pollutant molecules [3]. The uptake of uranyl ions from aqueous solutions has been attempted on a number of sorbents such as titanium oxide, aluminosilicates, silica, hematite sol, diatomite, etc. [4–6], the main focus being to achieve high sorption capacity in addition to selectivity [5]. Most of these sorbents, however, suffer from drawbacks such as small and irregular pore size, low surface area, poor selectivity, and inaccessible pores, thereby limiting their use to target such metal ions [6]. On the other hand, the mesoporous silicates, viz., one-dimensional hexagonal MCM-41 and three-dimensional cubic MCM-48, having remarkable features [7] such as large surface area ($\sim$1000 $m^2\ g^{-1}$), and tailored pore sizes with well-defined cylindrical pore shapes, thus show promise in the removal/entrapment of heavy metal ions from aqueous solutions. A number of methodologies have been adopted for this purpose, viz., functionalization of mesoporous materials in the removal of mercury [8], design of selective mesoporous anion traps in the removal of arsenic and chromium in the form of oxyanions [9], and the adsorption of UO_2^{2+} ions on calcined titanium based mesoporous materials [5].

We have recently reported the successful entrapment of uranyl ions in MCM-41 and MCM-48 molecular sieves following a direct-template-exchange method, wherein the template cations present in the mesopores were exchanged with the uranyl ions present in the aqueous solution [10,11]. In continuation of our earlier study, we have now investigated the effect of the pH of precursor uranyl nitrate solution on the sorption in mesoporous MCM-41 and MCM-48 molecular sieves. It is known that the process of sorption depends on a number of parameters [12], viz., properties of the uranyl ions (hydrolyzability), characteristics of the sorbents (point of zero charge), and experimental conditions such as the pH of uranyl solution and the concentration of uranyl ions. The main objective of the present study is to try to identify the uranyl species formed as a function of the pH of parent solution and to understand the role of these species in the overall sorption process. With this in view, the effect of solution pH on the nature of the sorbed uranyl species was monitored by FT-IR spectroscopy, while the amount of uranyl ions occluded was estimated by ICP-AES analysis. The physical and the crystallographic characteristics of the uranyl-exchanged samples were examined by powder X-ray diffraction (XRD) and nitrogen sorption isotherms.

2. Materials and methods

Fumed Silica (Aldrich; 99.8%), cetyltrimethylammonium bromide (CTAB; Lancaster; 98%) as surfactant, sodium hydroxide (Loba; 98%) as alkali source, and tetramethylammonium hydroxide (TMAOH; Aldrich; 25%) as organic base were used in the synthesis of MCM-41. Tetraethyl orthosilicate (TEOS; Aldrich; 98%), cetyltrimethylammonium bromide (CTAB; Lancaster; 98%), and sodium hydroxide (Loba; 98%) were used in the synthesis of MCM-48. Uranyl nitrate hexahydrate [$(UO_2)_2(NO_3)_2{\cdot}6H_2O$; Analytical] was used as a source of uranium.

MCM-41 and MCM-48 were synthesized according to a procedure described elsewhere [13]. In the synthesis of MCM-41, tetramethylammonium hydroxide was diluted with water and stirred for 10 min. To this, fumed silica was added slowly and a homogeneous 'Solution-A' was obtained. A 'Solution-B' was prepared by mixing cetyltrimethylammonium bromide (CTAB) and NaOH in distilled water, and the solution was stirred for about 30 min. Now, both 'Solution-A' and 'Solution-B' were mixed together

under constant stirring for an hour. The resulting gel was stirred further for an hour for homogenization. The typical gel (molar) composition was: SiO_2:0.27 CTAB:0.26 TMAOH:0.26 NaOH:68 H_2O.

In the synthesis of MCM-48, initially, a 'Solution-X' was obtained by mixing NaOH and tetraethylorthosilicate (TEOS) in distilled water under constant stirring for 10 min. A 'Solution-Y' was then prepared by dissolving CTAB in distilled water and was stirred for 20 min. Finally, a homogeneous transparent gel was obtained by mixing the 'Solution-X' and 'Solution-Y' under constant stirring for 25 min. The resulting gel was stirred further for an hour for homogenization. The typical gel (molar) composition was: SiO_2:0.6 CTAB:0.5 NaOH:60 H_2O. Finally, the pH of the gels was adjusted to 11.5 either by adding dilute H_2SO_4 or aqueous NaOH. The gels were crystallized in an air oven at 373 K for 1 and 3 days for MCM-41 and MCM-48, respectively, in Teflon-lined stainless steel autoclaves. The solid products obtained were washed, filtered and dried at 353 K. The resulting samples were designated as as-synthesized MCM-41 and MCM-48, respectively.

The uranyl-exchanged samples were obtained by contacting 1 g of as-synthesized MCM-41 and MCM-48 molecular sieves samples with 80 ml solution of 0.005 M uranyl nitrate with varying pH values in the range 1.40–8.60. The pH of the uranyl solution was adjusted with the help of either HNO_3, a buffer solution consisting of 0.26 CH_3COOH/0.54 CH_3COONa or alternately buffer pellets (Qualigens) of pH 9.00. The mixture was stirred using a magnetic stirrer at room temperature for duration of 12 h, followed by filtration, repeated washing with distilled water, and drying at 363 K for 10–12 h. These uranyl-exchanged samples were finally calcined at 823 K, initially for 2 h in nitrogen and then for 6 h in air. In order to monitor the changes in the mesoporous framework of the host matrix as a result of uranium occlusion, some experiments were also carried out on both the as-synthesized and the U-loaded MCM-41 and MCM-48 samples after subjecting them to calcination at 823 K for 2 h in nitrogen and then for 6 h in air.

Powder XRD patterns were recorded on a Rigaku diffractometer using a nickel-filtered copper Kα radiation. The scan speed and the step size were 0.5° min^{-1} and 0.02°, respectively. N_2 adsorption–desorption isotherms measurements were performed (on calcined samples) at 77 K using a Quantachrome Autosorb-1 unit. Prior to adsorption, the samples were evacuated at 523 K for 12 h. The surface area was estimated using the Brunauer–Emmett–Teller (BET) method and the pore size was calculated by Barrett–Joyner–Halenda (BJH) formula. The pore volume was determined from the amount of N_2 adsorbed at $P/P_0 = 0.5$. FT-IR spectra were recorded in the mid IR (4000–400 cm^{-1}) region using a Nicolet Impact 400 spectrometer at 4 cm^{-1} resolution. Compressed KBr pellets containing ~6 wt.% of a sample were employed for this purpose. Each spectrum was recorded on co-adding of 64 scans. The amount of uranium loaded in the samples was estimated by ICP-AES, using Labtam Plasma 8440 equipment. For this purpose, a known amount of calcined sample was placed in a weighed platinum crucible and was dissolved in aqua regia and then in 40% HF so as to obtain a clear solution. It was subsequently diluted with hot water for analysis.

3. Results and discussion

3.1. Effect of pH on the sorption of uranyl ions

As reported earlier [14], four kinds of uranyl species are known to exist in the pH range of 3.00–5.00; viz., UO_2^{2+}, $UO_2(OH)^+$, $(UO_2)_2(OH)_2^{2+}$, and $(UO_2)_3(OH)_5^+$, under the present experimental conditions. The relative concentration of these species however, depends on the pH and the concentration of uranyl

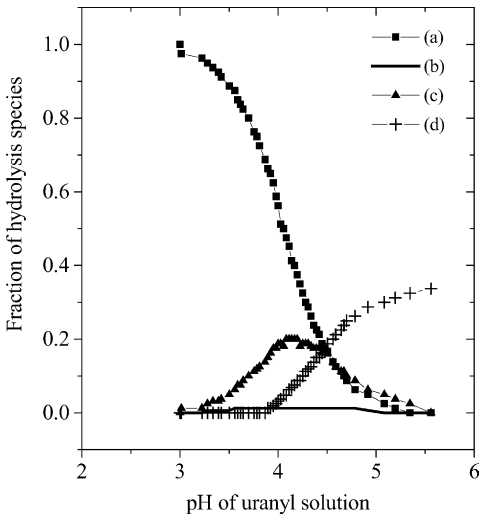

Fig. 1. Fraction of hydrolysis species of uranyl solution at a concentration of 0.005 M at 298 K: (a) UO_2^{2+}, (b) $UO_2(OH)^+$, (c) $(UO_2)_2(OH)_2^{2+}$, and (d) $(UO_2)_3(OH)_5^+$.

solution, the higher pH favoring the bulky or high nuclearity species, i.e., $(UO_2)_3(OH)_5^+$. Fig. 1 shows the effect of pH on the relative abundance of hydrolysis species in a uranyl solution of 0.005 M concentration at room temperature, as evaluated from literature data [14]. It can be seen that the hydrolysis of uranyl ions begins at a solution pH of ~3.00 and between pH 3.00 and 4.00, the uranyl ion, UO_2^{2+}, and its hydrolysis species, $UO_2{\cdot}OH^+$ and $(UO_2)_2(OH)_2^{2+}$ exist in different abundances. The formation of trinuclear uranyl species, $(UO_2)_3(OH)_5^+$ begins at pH ~4.00, and becomes dominant at pH >4.50. Fig. 2 depicts the amount of uranium occluded in the mesopores of MCM-41 and MCM-48 as a function of pH of the uranyl solution. It can be seen that the sorption of uranium increases with pH of the uranyl solution

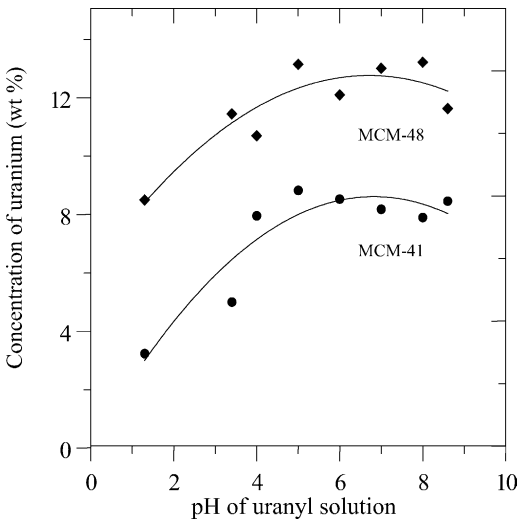

Fig. 2. Amount of uranium occluded in MCM-41 and MCM-48 as a function of pH of uranyl solution.

and reaches a maximum at around pH 5.00–6.00. This pH range corresponds to the formation of $(UO_2)_3(OH)_5^+$, and thus the maximum loading of uranium can be attributed to the formation of trinuclear, $(UO_2)_3(OH)_5^+$ species.

Further, the maximum amount of uranium occluded in MCM-48 (∼12.5%) is almost one and half times the amount occluded in MCM-41 (∼9.5%). This could be attributed to the higher surfactant content in MCM-48 (surfactant/silica = 0.60) as compared to MCM-41 (surfactant/silica = 0.27), which results in a higher exchange of uranyl ions [10,11]. Also, the diffusion of the $(UO_2)_3(OH)_5^+$ species is easier in the extensive network of the three-dimensional cubic MCM-48 than in the unidimensional channels of hexagonal MCM-41 [7,13,15]. Thus, the existence of an extensive three-dimensional pore system and higher surfactant content in cubic MCM-48 facilitates the easy diffusivity of the larger size hydrolysis species, as compared to the one-dimensional channels of the hexagonal MCM-41. This study also shows that a high loading of uranium depends not only on the type of uranyl species present at varying pH conditions, but also on the pore characteristics of the host matrix.

3.2. XRD studies

Figs. 3–6 show the powder XRD patterns of as-synthesized and uranyl-exchanged MCM-41 and MCM-48 samples. It can be seen from these figures that the uranyl-exchanged samples retain their parent structures [7,15,16] even after loading and subsequent treatments. Further, it is likely that if the exchanged uranyl ions preferentially reside in the mesopores, no considerable change in the unit cell dimension is expected. However, it is interesting to note that in the case of uranyl-exchanged MCM-41 samples (see Figs. 3 and 4; Table 1), the $d_{1\,0\,0}$-spacing values increase as compared to the non-exchanged

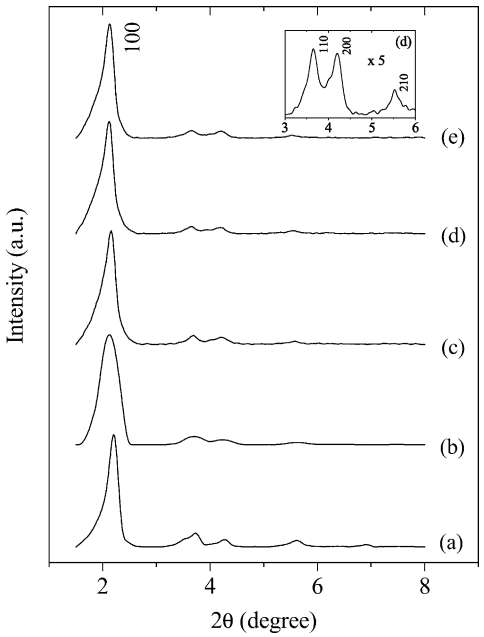

Fig. 3. Powder XRD patterns of (a) as-synthesized MCM-41 and uranyl exchanged MCM-41 at pH: (b) 1.40, (c) 3.45, (d) 4.00, (e) 5.00.

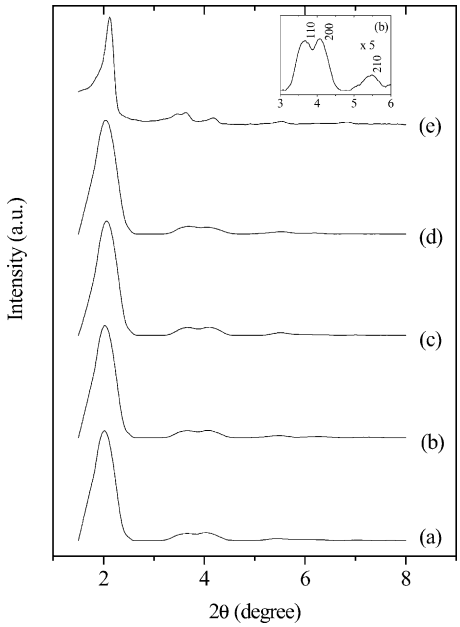

Fig. 4. Powder XRD patterns of uranyl exchanged MCM-41 at pH: (a) 6.00, (b) 7.00, (c) 8.00, (d) 8.60, and (e) UMCM-41 (Si/U = 500).

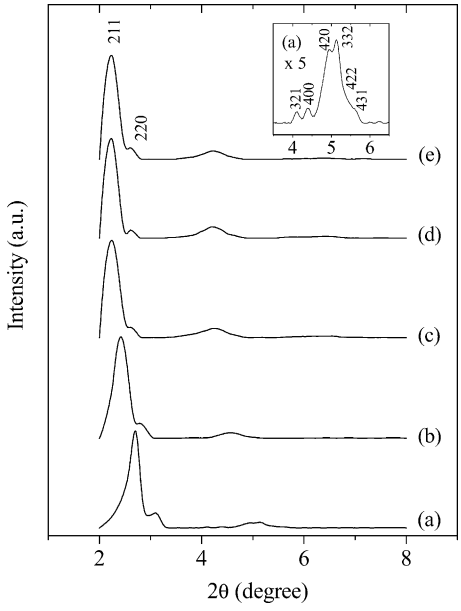

Fig. 5. Powder XRD patterns of (a) as-synthesized MCM-48 and uranyl exchanged MCM-48 at pH (b) 1.40, (c) 3.45, (d) 4.00, and (e) 5.00.

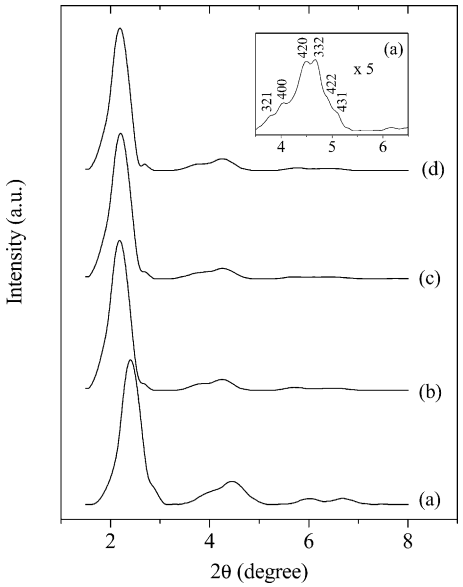

Fig. 6. Powder XRD patterns of uranyl exchanged MCM-48 at pH (a) 6.00, (b) 7.00, and (c) 8.00, and (d) 8.60.

parent MCM-41 sample ($d_{1\,0\,0}$ = 40.31 Å). A similar trend was also noticed for the MCM-48 structure where the $d_{2\,1\,1}$-spacing values showed an increase for the uranyl-exchanged samples (see Figs. 5 and 6) as compared to the parent MCM-48 sample ($d_{2\,1\,1}$ = 39.41 Å). The shifting of the reflections for these uranyl-exchanged samples may possibly be attributed to the partial isomorphous substitution of hexavalent uranium for the tetravalent silicon in the framework structure, i.e., UMCM-41 or UMCM-48. On this basis, this increase is quite understandable by considering the crystal radii of the ions in tetrahedral geometry ($r_{Si^{4+}} = 0.40$ and $r_{U^{6+}} = 0.66$ Å) [17].

This conjecture is well supported by the lattice expansion observed for trivalent iron, FeO(OH) or Fe_2O_3 nanoparticles, encapsulated in MCM-41 and MCM-48 structures [16,18], resulting in the formation of FeMCM-41 [19,20]. The substitution of heterometal ions such as aluminium and iron in the framework structure of mesoporous silicate materials is found to be facile under ambient (non-hydrothermal) synthesis

Table 1
Effect of uranyl solution pH on the *d*-spacing and FWHM of the uncalcined uranyl-exchanged MCM-41 and MCM-48 samples

pH of the uranyl solution	Uranyl exchanged MCM-41[a]		Uranyl exchanged MCM-48[b]	
	$d_{1\,0\,0}$ (Å)	FWHM (°)	$d_{2\,1\,1}$ (Å)	FWHM (°)
1.33	41.44(7)	0.33(1)	39.48(5)	0.33(2)
3.45	40.87(3)	0.24(2)	39.23(2)	0.34(2)
4.00	41.44(2)	0.24(2)	39.76(8)	0.32(1)
5.00	41.25(4)	0.24(3)	39.94(6)	0.33(1)
6.00	43.48(5)	0.40(2)	40.09(2)	0.45(2)
7.00	43.27(6)	0.40(1)	40.49(4)	0.44(1)
8.00	42.64(2)	0.40(1)	40.49(3)	0.44(2)
8.60	43.06(4)	0.42(2)	40.49(5)	0.44(2)

[a] For as-synthesized MCM-4, $d_{1\,0\,0}$ = 40.31(8) Å and FWHM = 0.21(1)°.
[b] For as-synthesized MCM-48, $d_{2\,1\,1}$ = 39.41(5) Å and FWHM = 0.30(1)°.

conditions [21–24]. Furthermore, FeMCM-41 prepared under hydrothermal conditions also showed evidence for the encapsulation as well as isomorphous substitution of trivalent iron in MCM-41 [25]. In addition, it also noteworthy that a similar shift in the main reflection ($d_{1\,0\,0}$ = 42.035 Å) compared to the parent MCM-41 sample (see Fig. 4e) was observed in case of a hydrothermally synthesized UMCM-41 sample (Si/U = 500), as reported in our earlier study [26]. It can also be seen from Table 1 that the full width at half maximum (FWHM) values of the uranyl-exchanged samples show an increase at pH values greater than 5. Figs. 4 and 6 show broadening of the 1 0 0 and 2 1 1 reflections at pH >5.00 for uranyl exchanged MCM-41 and MCM-48, respectively. This could possibly be attributed to the formation of trinuclear uranyl species, $(UO_2)_3(OH)_5^+$, formed at pH >5.00. It is surmised that the in-situ formation of these bulky hydrolysis species in the mesopores of MCM-41 and MCM-48 may lead to the destruction of the mesopore wall structure. In other words, the samples lose their crystallinity partially when solutions of high pH are involved, due to the formation of the bulky hydrolysis species.

3.3. FT-IR studies

Figs. 7 and 8 depict the FT-IR spectra of uranyl exchanged MCM-41 at various pH of uranyl nitrate solution employed for exchange. For a comparison, Fig. 8e shows the spectrum of UMCM-41

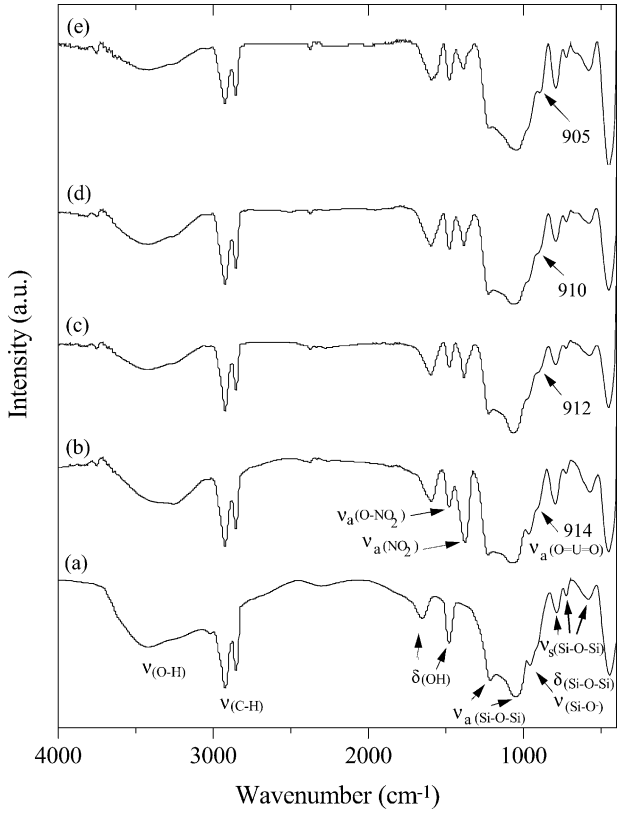

Fig. 7. FT-IR spectra of (a) as-synthesized MCM-41 and uranyl exchanged MCM-41 at pH (b) 1.4, (c) 3.45, (d) 4.00, and (e) 5.00.

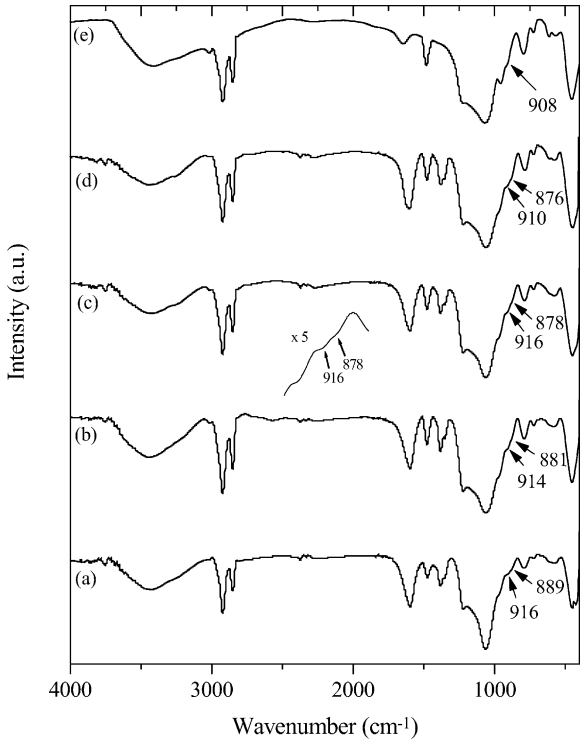

Fig. 8. FT-IR spectra of uranyl exchanged MCM-41 at pH (a) 6.00, (b) 7.00, (c) 8.00, (d) 8.60, and (e) UMCM-41 (Si/U = 500).

(Si/U = 500), prepared by hydrothermal synthesis. Similarly, Figs. 9 and 10 show the FT-IR spectra of uranyl exchanged MCM-48 at various pH of the uranyl solution. Figs. 7a and 9a are the FT-IR spectra of the parent or as-synthesized MCM-41 and MCM-48 samples. The assignment of the various bands is as follows: In the as-synthesized samples, the bands between 3200–3600 cm^{-1} correspond to the ν_{O-H} vibrations and those at around 2920 and 2848 cm^{-1} correspond to the ν_{C-H} of the surfactant, CTA^+ [27,28]. The bands around 1230 and 1060 cm^{-1} are due to ≡Si–O–Si≡ asymmetric stretching, ν_a(Si–O–Si), whereas, the bands at 794, 725, and 590 cm^{-1} arise due to ≡Si–O–Si≡ symmetric stretching ν_s(Si–O–Si). The band at 459 cm^{-1} may be assigned to ≡Si–O–Si≡ bending ($\delta_{Si-O-Si}$) vibration. The bands in the range 1700–1300 cm^{-1} are due to δ_{O-H}. All these bands are characteristic of the mesoporous silicate framework [28] (cf. Figs. 7a and 9a). In the case of uranyl exchanged samples, the bands at around 1481, 1390, and 727 cm^{-1} are due to ν_a(O–NO_2), ν_a(NO_2), and δ(NO_2) vibrations, respectively [27] as seen in Figs. 7b and 9b. In addition, the IR band at ∼914 cm^{-1} as seen in Fig. 7b corresponds to asymmetric stretching vibration, ν_a(U=O) of the axial O=U=O group [28]. The frequency of this band was found to decrease progressively with the increasing pH of uranyl solution, as seen in Figs. 7–10.

As reported earlier [29], the nature of complexes formed during the hydrolysis of uranyl ions depends on the pH of the uranyl solution. For example, a decrease in ν_a(U=O) was observed from 910 to 905 cm^{-1} for a uranium loaded hematite sol when the pH of the parent solution employed for preparing the sample increased from 4.30 to 6.08 [29]. This was ascribed to the formation of trinuclear hydrolysis species, $(UO_2)_3(OH)_5^+$, at pH = 6.08. In the present study, at pH 1.30–5.00, Fig. 7 shows a decrease in the ν_a(U=O) from 914 to 905 cm^{-1} for uranyl exchanged MCM-41. Similarly, Fig. 9 shows a decrease in the axial

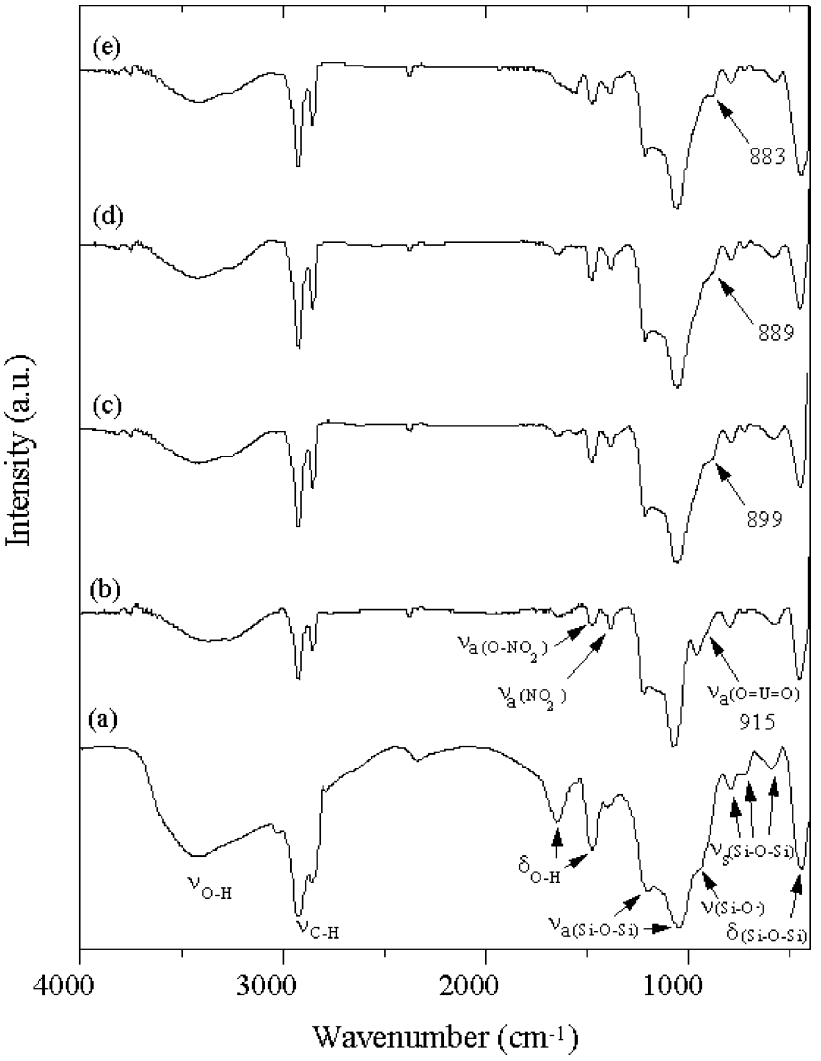

Fig. 9. FT-IR spectra of (a) as-synthesized MCM-48 and uranyl exchanged MCM-48 at pH (b) 1.40, (c) 3.45, (d) 4.00, and (e) 5.00.

O=U=O stretching frequency from 915 to 883 cm^{-1} for uranyl exchanged MCM-48 samples in the same pH range. This could thus be attributed to the formation of the high nuclearity hydrolysis species, which is expected to result in the weakening of the axial O=U=O bonds. This weakening can be explained by the overlap of ligand orbitals (hydroxyl) with the ϕ_u and d_u orbitals of uranium (non-bonding), which leads to an accumulation of excess negative charge on uranium. Thus, a repulsion between the excess negative charge on uranium and the axial oxygen atoms may lead to the weakening of the O=U=O band, and hence a decrease in frequency of $\nu_{U=O}$ vibration is observed [30]. For samples prepared from uranyl solutions of pH >5, the presence of two bands at ~920 and ~879 cm^{-1} can be observed in spectra a–d of Figs. 8 and 10. It has been reported [31] that if the uranyl ion lacks a centre of symmetry (the uranyl ion is not linear, but bent), the Raman and Infrared are no longer mutually exclusive, and thus the O=U=O symmetric

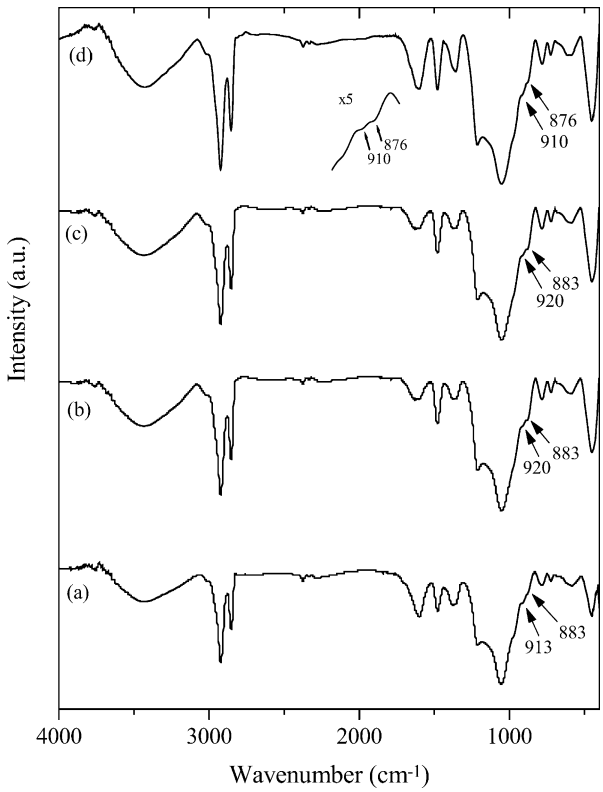

Fig. 10. FT-IR spectra of uranyl exchanged MCM-48 at pH (a) 6.00, (b) 7.00, (c) 8.00, and (d) 8.60.

stretching, ν_s(U=O), the asymmetric stretching, ν_a(U=O), and bending vibrations, $\delta_{U=O}$ should appear in both. Thus, it is possible that the formation of the trinuclear hydrolysis species, $(UO_2)_3(OH)_5^+$, destroys the centre of symmetry around the uranyl ion, $[O=U=O]^{2+}$, and gives rise to the symmetric O=U=O stretching frequency, ν_s(U=O) at $\sim$879 cm^{-1}, in addition to the asymmetric stretching frequency, ν_a(U=O) at $\sim$920 cm^{-1}.

Fig. 11 depicts the plot of the ratio of intensities of ν_{C-H} (2920 cm^{-1}) and $\nu_{a(Si-O-Si)}$ (1060 cm^{-1}), A_{2920}/A_{1060}, versus the pH of the uranyl solution employed for the uranyl exchanged MCM-41 and MCM-48 samples. It can be seen that with increase in pH of uranyl solution from 1.30 to 3.45, an increase in the A_{2920}/A_{1060} takes place. From pH 4.00–6.00, there is a further increase in the A_{2920}/A_{1060}, after which it becomes constant. From our earlier studies [10,11], we demonstrated by FT-IR that the surfactant content present in the mesopores of MCM-41 and MCM-48, ν_{C-H} decreased as a function of exchange time of uranyl ions, and the decrease was proportional to the increase in the uranium sorption. However, in the present investigation, an increase in the surfactant content (reflected by a higher A_{2920}/A_{1060}) in the mesopores of uranyl exchanged MCM-41 and MCM-48 is observed, which is proportional to an increase in uranium sorption (see Fig. 2). This different behaviour could be attributed to the formation of uranyl hydrolysis species. Thus, at pH 1.30, uranyl ion, present as the UO_2^{2+} (average diameter = 3.6 Å [32]) results in a large exchange, which is reflected in a small A_{2920}/A_{1060} value for uranyl-exchanged MCM-41 and MCM-48 as compared to the parent samples (A_{2920}/A_{1060} = 0.701 for MCM-41 and 0.810 for MCM-48). From pH 3.45 to 4.00, an increase in A_{2920}/A_{1060} is observed, thus

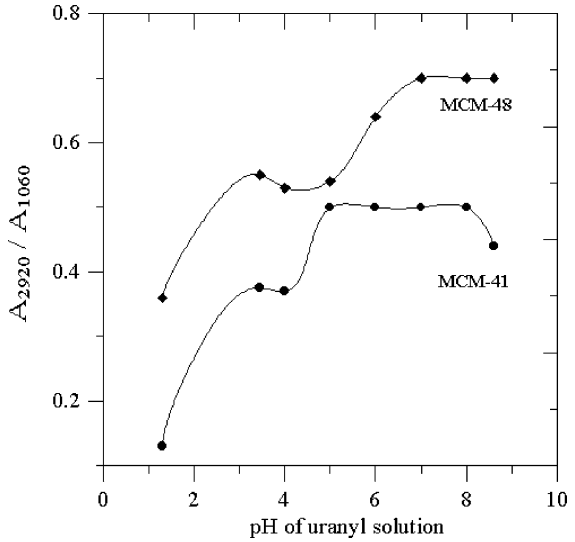

Fig. 11. Ratio of relative intensities of ν_{C-H} and ν_a(Si–O–Si), (A_{2920}/A_{1060}) with respect to pH of uranyl solution.

indicating that lesser amount of surfactant, CTA^+ has been exchanged. This could be attributed to the smaller charge to size ratio of the dinuclear species, $(UO_2)_2(OH)_2^{2+}$ present, in addition to UO_2^{2+}, as seen in Fig. 1, thus resulting in a lesser exchange. Further, from pH 4.00 to 5.00, a further increase in A_{2920}/A_{1060} is observed, which becomes constant at pH ~6.00. The trinuclear species, $(UO_2)_3(OH)_5^+$, present at pH >4.50, has an average diameter of 10–11 Å [33], which results in a further decrease in the charge to size ratio of the cation, and hence a lesser exchange of the surfactant. Hence a further increase in the A_{2920}/A_{1060} can be observed. Thus, this supports the formation of trinuclear species, $(UO_2)_3(OH)_5^+$ at pH >5.00 as seen in XRD studies, ICP-AES analysis, and FT-IR spectroscopy.

3.4. Effect of calcination

Table 2 presents the XRD and N_2 adsorption data on the effect of calcination on the physico-chemical characteristics of parent MCM-41/ MCM-48 materials and also the corresponding uranyl-exchanged and calcined samples, synthesized at the optimum pH of 5.00. It can be seen from the results in Table 2 that the *d*-spacing values decrease considerably on calcination, as compared to the as-synthesized and uranyl-

Table 2
Physico-chemical characteristics of MCM-41/MCM-48 and corresponding uranyl-exchanged samples (synthesized at pH = 5.00), subjected to identical treatment of calcination at 823 K first under N_2 and then under air

Sample	*d* (Å)	a_0 (Å)	BET surface area ($m^2\ g^{-1}$)	Mean pore diameter (Å)	Pore volume ($ml\ g^{-1}$)
Calcined MCM-41	$d_{1\,0\,0}$ = 35.30(5)	40.76(6)	1032(14)	28.2(5)	0.90(5)
Uranyl-exchanged and calcined MCM-41	$d_{1\,0\,0}$ = 37.10(7)	42.84(7)	612(20)	27.0(5)	0.65(4)
Calcined MCM-48	$d_{2\,1\,1}$ = 34.90(3)	85.50(3)	1189(16)	26.6(7)	1.05(2)
Uranyl-exchanged and calcined MCM-48	$d_{2\,1\,1}$ = 36.03(5)	88.27(5)	590(20)	23.8(6)	0.50(4)

exchanged samples. This could easily be attributed to the removal of template ions and the decomposition of remnant uranyl nitrate molecules in the pore system. Further, an increase in the *d*-spacing and average unit cell parameter (a_0) of the uranium containing samples was observed as compared to parent MCM-41/MCM-48 subjected to similar calcination, which could be attributed to the partial isomorphous substitution of hexavalent uranium in the mesoporous matrix, as discussed earlier. We may also notice in Table 2 that the pore size, pore volume and the surface area of the uranium containing sample is lower than that of the corresponding MCM-41/MCM-48 sample subjected to identical calcination treatment. These features may be attributed to the presence of uranyl species and other uranium oxide moieties within the pores of MCM-41 and MCM-48. Our earlier reported studies have indeed demonstrated that the calcination of the uranyl-exchanged MCM-41 and MCM-48 samples resulted in the partial transformation of the uranyl species to uranium oxide moieties, the framework mesoporous structure remaining intact [3,10,11].

4. Conclusions

The uptake of uranyl ions in mesoporous MCM-41 and MCM-48 was investigated as a function of the pH of uranyl solution. The formation of high nuclearity, $(UO_2)_3(OH)_5^+$ type species was responsible for the higher loading in MCM-41 and MCM-48. The amount of uranium loaded in MCM-41 (9.5 wt.%) was found to be almost one and a half times that of the amount sorbed in MCM-48 (12.5 wt.%), which was attributed to the higher surfactant content in MCM-48 than in MCM-41, in addition to the pore structure characteristics. The presence of an extensive three-dimensional pore system in MCM-48 facilitates the easy diffusion of the bulky species, compared to the diffusion in the one-dimensional pore system in MCM-41. XRD studies revealed a partial substitution of hexavalent uranium (isomorphous) along with broadening of the reflections with increasing pH of parent solution indicating the influence of bulky hydrolysis species in the mesopores of MCM-41 and MCM-48. FT-IR studies revealed a decrease in the $\nu_{U=O}$ of the axial O=U=O band with an increase in the pH of uranyl solution. This could again be attributed to the formation of hydrolysis species accompanied with the weakening of the axial O=U=O bonds. The presence of two $\nu_{U=O}$ bands at ~920 and ~879 cm^{-1} due to the appearance of both asymmetric and symmetric O=U=O stretching frequencies at uranyl solutions of pH >5.00 support the formation of high nuclearity species. Also, the increase in the A_{2920}/A_{1060} with increasing pH provides further evidence regarding the formation of $(UO_2)_3(OH)_5^+$ species at pH >5.00. The present study thus indicates that the sorption of uranium in mesopores of MCM-41 and MCM-48 depends not only on the hydrolysis species of the uranyl ion, but also on the pore characteristics of the host matrix. The XRD and the nitrogen adsorption−desorption data further revealed that the calcination of uranium containing samples resulted in narrowing of pores in the host matrix owing to the occlusion of uranium oxide species.

Acknowledgements

The authors thank RSIC, IIT-Bombay for ICP-AES analysis This work is supported by the Board of Research in Nuclear Sciences (BRNS), Department of Atomic Energy, Mumbai, under a Contract No. 99/37/31/BRNS/1049.

References

[1] S.L. Suib, A. Kostapapas, D. Psaras, J. Am. Chem. Soc. 106 (1984) 1614.
[2] S.L. Suib, K.A. Carrado, Inorg. Chem. 24 (1985) 863.
[3] D. Kumar, K. Vidya, P. Selvam, G.K. Dey, N.M. Gupta, in: A. Sharma, J. Bellare, A. Sharma (Eds.), Advances in Nanoscience Nanotechnology, NISCOM, New Delhi, 2004, p. 265.
[4] M.T. Olguin, M. Solache-Rios, D. Acosta, P. Bosch, S. Bulbulian, Micropor. Mesopor. Mater. 28 (1999) 377.
[5] Y. Shin, M.C. Burleigh, S. Dai, C.E. Barnes, X.L. Xue, Radiochim. Acta 84 (1999) 37.
[6] L. Mercier, T.J. Pinnavaia, Adv. Mater. 9 (1997) 500.
[7] J.S. Beck, J.C. Vartuli, W.J. Roth, M.E. Leoniwicz, K.D. Schmidtt, C.D.-W. Chu, D.H. Olson, E.W. Sheppard, S.B. McCullen, J.B. Higgins, J.L. Schlenker, J. Am. Chem. Soc. 114 (1992) 10834.
[8] J. Liu, X. Feng, G.E. Fryxell, L.-Q. Wang, A.Y. Kim, M. Gong, Adv. Mater. 10 (1998) 161.
[9] G.E. Fryxell, J. Liu, T.A. Hauser, Z. Nie, K.F. Ferris, S. Mattigod, M. Gong, R.T. Hallen, Chem. Mater. 11 (1999) 2148.
[10] K. Vidya, S.E. Dapurkar, P. Selvam, S.K. Badamali, N.M. Gupta, Micropor. Mesopor. Mater. 50 (2001) 173.
[11] K. Vidya, S.E. Dapurkar, P. Selvam, S.K. Badamali, D. Kumar, N.M. Gupta, J. Mol. Catal. A 181 (2002) 91; K. Vidya, S.E. Dapurkar, P. Selvam, S.K. Badamali, D. Kumar, N.M. Gupta, J. Mol. Catal. A 191 (2003) 149.
[12] A.R. Gupta, B. Venkataramani, Bull. Chem. Soc. Jpn. 61 (1988) 1357.
[13] S.E. Dapurkar, S.K. Badamali, P. Selvam, Catal. Today 68 (2001) 63.
[14] N. Mikami, M. Sasaki, K. Hachiya, T. Yasunaga, J. Phys. Chem. 87 (1983) 5478.
[15] P. Selvam, S.K. Bhatia, C. Sonwane, Ind. Eng. Chem. Res. 40 (2001) 3237.
[16] S.E. Dapurkar, P. Selvam, Mater. Phys. Mech. 4 (2001) 13.
[17] R.D. Shannon, Acta Crystallogr. A 32 (1976) 751.
[18] P. Selvam, S.E. Dapurkar, S.K. Badamali, M. Murugesan, H. Kuwano, Catal. Today 68 (2001) 69.
[19] S.K. Badamali, P. Selvam, Stud. Surf. Sci. Catal. 113 (1998) 749.
[20] S.K. Badamali, A. Sakthivel, P. Selvam, Catal. Lett. 65 (2000) 153.
[21] H. Hamdan, S. Endud, H. He, M.N.N. Muhid, J. Klinowski, J. Chem. Soc., Faraday Trans. 92 (1996) 2311.
[22] K. Schumacher, M. Grun, K.K. Unger, Micropor. Mesopor. Mater. 27 (1999) 201.
[23] N.Y. He, J.M. Cao, S.L. Bao, Q.H. Xu, Mater. Lett. 31 (1997) 133.
[24] A. Tuel, I. Arcon, J.M.M. Millet, J. Chem. Soc., Faraday Trans. 94 (1998) 3501.
[25] P. Selvam, S.K. Badamali, M. Murugesan, H. Kuwano, in: V. Murugesan, B. Arabindoo, M. Palanichamy (Eds.), Recent Trends in Catalysis, Narosa, New Delhi, 1999, p. 556.
[26] D. Kumar, K.T. Pillai, V. Sudersanan, G.K. Dey, N.M. Gupta, Chem. Mater. 15 (2003) 3859.
[27] H.A. Szymanski, Progress in IR Spectroscopy, Plenum Press, New York, 1962.
[28] K. Nakamoto, Infrared and Raman Spectra of Inorganic and Coordination Compounds, Wiley, New York, 1978.
[29] C.H. Ho, D.C. Doern, Can. J. Chem. 63 (1985) 1100.
[30] L.M. Toth, G.M. Begun, J. Phys. Chem. 85 (1981) 547.
[31] S.P. McGlynn, J.K. Smith, J. Mol. Spectr. 6 (1961) 164.
[32] P.C. Burns, R.C. Ewing, F.C. Hawthorne, Can. Mineralogist 35 (1997) 1551.
[33] P. Michard, E. Guibal, T. Vincent, P. Le Cloirec, Micropor. Mater. 5 (1996) 309.